Journal of Elasticity **68:** 95–121, 2002.

Classification of the Spatial Equilibria of the Clamped Elastica: Symmetries and Zoology of Solutions

SÉBASTIEN NEUKIRCH[1,⋆] and MICHAEL E. HENDERSON[2]
[1]*Bernoulli Institute, School of Basic Sciences, École Polytechnique Fédérale de Lausanne, CH-1015 Lausanne, Switzerland. E-mail: sebastien.neukirch@epfl.ch*
[2]*T.J. Watson Research Center I.B.M., Yorktown Heights, NY 10598, U.S.A. E-mail: mhender@us.ibm.com*

Received 12 November 2002; in revised form 2 April 2003

Abstract. We investigate the configurations of twisted elastic rods under applied end loads and clamped boundary conditions. We classify all the possible equilibrium states of inextensible, unshearable, isotropic, uniform and naturally straight and prismatic rods. We show that all solutions of the clamped boundary value problem exhibit a π-flip symmetry. The Kirchhoff equations which describe the equilibria of these rods are integrated in a formal way which enable us to describe the boundary conditions in terms of 2 closed form equations involving 4 free parameters. We show that the flip symmetry property is equivalent to a reversibility property of the solutions of the Kirchhoff differential equations. We sort these solutions according to their period in the phase plane. We show how planar untwisted configurations as well as circularly closed configurations play an important role in the classification.

Mathematics Subject Classifications (2000): 74B20, 74K10, 74G05, 74G60, 37J35, 70K42, 34B08.

Key words: classification of boundary value problem solutions for elastic rods.

1. Introduction

We study equilibrium solutions of long and thin elastic rods. We use the Cosserat rod theory [1] to describe the state of the rod (also called a configuration) by its centre line together with a field of directors: at each point along the centre line curve, a set of 3 orthogonal unit vectors, the directors, provides a way to describe local bending, twisting, stretching and shearing of the elastic material. Constitutive relations express the way these elastic deformations are related to the stresses in the rod.

We restrain our study to a non-shearable and non-extensible rod, namely, an elastica. Under the further assumptions of hyper-elasticity (existence of a strain energy from which the stresses are derived) and linear constitutive relations (i.e. the strain energy is a quadratic function of the strains) we have a Kirchhoff elastica

⋆ Corresponding author.

[18, 14]. Here we only consider what we call the *ideal elastica*, i.e. a Kirchhoff elastica made of an isotropic material with symmetrical cross section, that has uniform elastic rigidities and that is straight and prismatic in its unstressed state. The name elastica is attached to the work of Euler [9] where twistless planar configurations have been classified. Our goal here is to classify all the possible equilibrium states of the twisted spatial ideal elastica when subjected to clamped (a special case of strong anchoring) boundary conditions: a rod held by its two ends where both tangents are aligned with each other (see Figure 2).

As it has been shown in various works [12, 16, 23, 22, 25], the equilibrium equations of the ideal elastica are integrable and closed form solutions can be written for its shape. Nevertheless the parameters used there (e.g., roots of a third degree polynomial or modulus of elliptic integrals) were not easily related to physical parameters (e.g., force, moment, deflection angle). This and the use of Euler angles makes continuation of solutions awkward. In [21] integrals of motion were used as parameters which enable the authors to make a first step toward a general geometric classification of the equilibrium solutions. Still solutions remained implicitly defined by the roots of a third degree polynomial.

The paper is organized as follows: we first recall the Kirchhoff equations that govern the equilibrium of the elastica and we show how these equations in the case of the ideal elastica can be reduced to a set of 2 vectorial ordinary differential equations that describe its centre line, the arc-length playing the role of the independent variable. We then describe the clamped boundary conditions and write two equations the centre line has to fulfill in order to meet them (Section 3).

We then further reduce the system of equations to an equivalent oscillator (as introduced in [1] and used in [26]) and show how clamped boundary conditions select only reversible solutions of this conservative system. We use a new set of parameters which are easily related to physical quantities. Then we derive closed form solutions for the Cartesian coordinates of the centre line in which the parameters appear explicitly. We next write the clamped boundary conditions as two equations for these parameters. We also show that closed trajectories of the phase plane either correspond to planar twistless configurations (planar elastica) or circularly closed configurations (i.e., *rings*, Section 3).

Using the frequency of the trajectories in the phase plane, we classify the possible solutions by labeling them with an integer and a sign and we show that in order to change the label, one has to deform the solution such that it passes through a ring (Section 4).

2. The Model

2.1. THE KIRCHHOFF STATIC EQUATIONS

We study the equilibrium of a rod of length L when subjected to external forces and moments. The force $\boldsymbol{F}$ and moment $\boldsymbol{M}$ balance equations for an infinitesimal

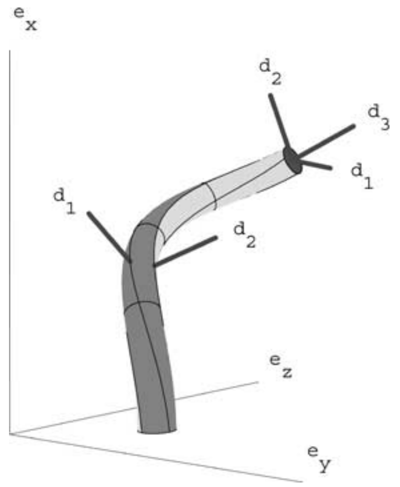

Figure 1. A twisted elastic rod. The drawn lines along the rod enable us to follow the twist. The directors frame $\boldsymbol{d_i}$ is also shown at two different arc-length positions.

cross-section element of the rod centre line $\{\boldsymbol{R}(S) S \in [0, L]\}$ are given by [1]:

$$\boldsymbol{F}' = \boldsymbol{0}, \tag{1}$$

$$\boldsymbol{M}' + \boldsymbol{R}' \times \boldsymbol{F} = \boldsymbol{0}, \tag{2}$$

where S denotes arc-length along the rod, and $(\ )' \stackrel{\text{def}}{=} \mathrm{d}/\mathrm{d}S$. We first note that the internal force $\boldsymbol{F}$ is constant along the rod. Apart from the fixed frame $\{\boldsymbol{e_x}, \boldsymbol{e_y}, \boldsymbol{e_z}\}$, we define a right-handed rod-centered orthonormal co-ordinate frame $\{\boldsymbol{d}_1, \boldsymbol{d}_2, \boldsymbol{d}_3\}$. In the case of an inextensible, unshearable rod the vector $\boldsymbol{d}_3$ is the local tangent to the rod and $\boldsymbol{d}_1$ and $\boldsymbol{d}_2$ are two vectors in the normal cross-section that enable one to follow the twist as we travel along the rod. We have:

$$\boldsymbol{R}' = \boldsymbol{d}_3, \tag{3}$$

while the evolution of the orthonormal frame $\boldsymbol{d}_i$ along the rod is governed by the equation

$$\boldsymbol{d}_i' = \boldsymbol{U} \times \boldsymbol{d}_i, \quad i = 1, 2, 3. \tag{4}$$

Here $\boldsymbol{U}$ is the strain vector whose components in the moving frame are the curvatures and the twist. In order to close the system of equations, we have to introduce constitutive relations that relate the moments $M_i = \boldsymbol{M} \cdot \boldsymbol{d}_i$ to the strains $U_i = \boldsymbol{U} \cdot \boldsymbol{d}_i$. The assumption of hyper-elasticity introduces a strain energy $W(Q_i)$ from which the moments M_i are partial derivatives:

$$M_i = \left.\frac{\partial W}{\partial Q_i}\right|_{Q_i = U_i(s) - \widehat{U}_i(s)}.$$

The Kirchhoff theory of linear elastic rods [18] uses a strain energy that is quadratic in the strains, implying

$$M_i = \sum_{j=1}^{j=3} K_{ij}(S)(U_j(S) - \widehat{U}_j(S)), \tag{5}$$

where K_{ij} is a positive definite matrix. In the case of a rod which is straight and prismatic in its unstressed state we have $\widehat{U}_j(s) \equiv 0$. In the case of uniform elastic properties along the rod, we have constant K_{ij}'s. We further simplify our study by only considering the diagonal case $K_{ij} = 0$ if $i \neq j$ and note $K_i \stackrel{\text{def}}{=} K_{ii}$. Then (5) becomes

$$M_i = K_i U_i. \tag{6}$$

We refer to K_1 and K_2 as the bending rigidities and to K_3 as the torsional rigidity. From now on, we only consider rods with isotropic cross sections, i.e. $K_1 = K_2 \stackrel{\text{def}}{=} K_0$.

We have then 7 unknown vector functions $\boldsymbol{F}$, $\boldsymbol{M}(S)$, $\boldsymbol{R}(S)$, $\boldsymbol{d}_1(S)$, $\boldsymbol{d}_2(S)$, $\boldsymbol{d}_3(S)$, $\boldsymbol{U}(S)$ and 6 vectorial ordinary differential equations (1)–(4) and a relation between 3 components (6). This relation (6) involves components of vectors in the moving frame. Hence in the general case, the vectorial ordinary differential equations (1)–(4) have to be written in the moving frame as well.

2.2. NON-DIMENSIONALIZATION

We are interested in rods of finite length L. The case where the length is infinite as been studied in [26] and comparison of stability between finite and infinite length in [20]. We normalize the physical quantities using L and K_0:

$$\boldsymbol{f} \stackrel{\text{def}}{=} \frac{\boldsymbol{F}}{K_0}\left(\frac{L}{2\pi}\right)^2, \qquad \boldsymbol{m} \stackrel{\text{def}}{=} \frac{\boldsymbol{M}}{K_0}\left(\frac{L}{2\pi}\right), \qquad \boldsymbol{u} \stackrel{\text{def}}{=} \boldsymbol{U}\left(\frac{L}{2\pi}\right), \tag{7}$$

$$\boldsymbol{r} \stackrel{\text{def}}{=} \boldsymbol{R}\left(\frac{2\pi}{L}\right), \qquad s \stackrel{\text{def}}{=} S\left(\frac{2\pi}{L}\right), \qquad \gamma \stackrel{\text{def}}{=} \frac{K_3}{K_0} \tag{8}$$

with $\dot{(\,)} \stackrel{\text{def}}{=} \mathrm{d}/\mathrm{d}s$. The integration of the differential equations will be carried over a range of 2π for s.

2.3. REDUCTION OF THE SYSTEM

Since we only consider boundary conditions (see Section 2.4) that involves the centre line together with its tangent, we are only interested in integrating equations (3) and (4) with $i = 3$. In the general case we would have followed the scheme introduced in [5] that reduce the problem to a 7 degrees Hamiltonian system (14 ODEs). Nevertheless here using the symmetry properties we follow another scheme that reduce the problem to a system of 6 ODEs.

Equation (1) yields $\boldsymbol{f} = constant$. Then equation (2) can be integrated to give

$$\boldsymbol{m}(s) = \boldsymbol{f} \times \boldsymbol{r}(s) + \boldsymbol{m}_K, \tag{9}$$

where $\boldsymbol{m}_K$ is an integration constant which takes $\boldsymbol{r}(0)$ into account. It also shows that $I_0 \stackrel{\text{def}}{=} \boldsymbol{m}(s) \cdot \boldsymbol{f}$ is a constant of s. Furthermore, from equations (2)–(4) and (6) (with $K_1 = K_2$), we have that the twisting moment along the rod $m_3 \stackrel{\text{def}}{=} \boldsymbol{m} \cdot \boldsymbol{d_3}$ is also constant.

Next we show how $\boldsymbol{U}$ can be replaced by $\boldsymbol{M}$ in equation (4) with $i = 3$. We first introduce $\boldsymbol{u}_\parallel \stackrel{\text{def}}{=} (\boldsymbol{u} \cdot \boldsymbol{d_3})\boldsymbol{d_3}$ and $\boldsymbol{u}_\perp \stackrel{\text{def}}{=} \boldsymbol{u} - \boldsymbol{u}_\parallel$ and note that

$$\boldsymbol{m}_\parallel = \gamma \boldsymbol{u}_\parallel \quad \text{hence } \boldsymbol{u}_\parallel = \frac{m_3}{\gamma}\boldsymbol{d_3}. \tag{10}$$

More importantly we have $\boldsymbol{m}_\perp = \boldsymbol{u}_\perp$ which means that the constitutive relation (6) can be written as a vectorial equation (instead of a relation between components, see [24, 21]):

$$\boldsymbol{m} = \boldsymbol{u}_\perp + \gamma \boldsymbol{u}_\parallel = \boldsymbol{d_3} \times \dot{\boldsymbol{d}}_3 + m_3\boldsymbol{d_3}. \tag{11}$$

This enables us to write equation (4) with $i = 3$ in a form not involving $\boldsymbol{u}$:

$$\dot{\boldsymbol{d}}_3 = \boldsymbol{u} \times \boldsymbol{d_3} = \boldsymbol{u}_\perp \times \boldsymbol{d_3} = \boldsymbol{m}_\perp \times \boldsymbol{d_3} = \boldsymbol{m} \times \boldsymbol{d_3} \tag{12}$$

and this gives us the system of 2 vectorial ordinary differential equations for the centre line of the ideal elastica:

$$\dot{\boldsymbol{r}} = \boldsymbol{d_3}, \tag{13}$$
$$\dot{\boldsymbol{d}}_3 = (\boldsymbol{f} \times \boldsymbol{r} + \boldsymbol{m}_K) \times \boldsymbol{d_3} \tag{14}$$

with the following integrals of motion:

$$\boldsymbol{d}_3 \cdot \boldsymbol{d}_3 = 1, \tag{15}$$
$$I_1 \stackrel{\text{def}}{=} (\boldsymbol{f} \times \boldsymbol{r} + \boldsymbol{m}_K) \cdot \boldsymbol{d_3}\ (= m_3) = constant, \tag{16}$$
$$I_2 \stackrel{\text{def}}{=} \frac{1}{2}|(\boldsymbol{f} \times \boldsymbol{r} + \boldsymbol{m}_K)|^2 + \boldsymbol{d}_3 \cdot \boldsymbol{f} = constant. \tag{17}$$

There are two ways to handle equations (13) and (14). The first way is to further reduce the system by using the integrals of motion and introducing Euler angles (see Section 3.1). The second way is to consider equations (13) and (14) as a set of 6 ordinary differential equations. These are quadratic polynomials in the components and do not have the continuity and definition problems one can encounter with Euler angles. We will use them while performing the numerical continuation of solution [10]. In this scheme a rod configuration will depend on both parameters $(\boldsymbol{f}, \boldsymbol{m}_K)$ and initial conditions $(\boldsymbol{d_3}(0), \boldsymbol{r}(0))$. In order to simplify the study, we perform certain choices that do not reduce the generality:

- We choose the origin of the arc-length such that the point $\boldsymbol{r}(0)$ lies at the middle of the rod, i.e. $s \in [-\pi; +\pi]$. This will prove very useful in the presence of symmetries.
- We choose the origin of the fixed frame such that $\boldsymbol{r}(0) = 0$ (then $\boldsymbol{m}_K = \boldsymbol{m}(0)$).
- The case $\boldsymbol{f} = 0$ being treated in Table II, in the case of non null force we choose the $\boldsymbol{e_z}$ axis along and in the direction of $\boldsymbol{f} = (0, 0, f > 0)$. The integral of motion I_0 becomes $I_0 = f m_z$, with m_z constant.
- We choose the $\boldsymbol{e_x}$ and $\boldsymbol{e_y}$ axis such that the rod at $s = 0$ lies in the $(\boldsymbol{e_x}, \boldsymbol{e_z})$ plane (i.e. $d_{3y}(0) = 0$). This selects 2 isolated solutions (with $f > 0$) among the degenerated manifold of possible solutions consisting in rotations around the axis $\boldsymbol{\ell}$ of Figure 2 (see also Figure 3 of [2]).

Note that in the present case of an ideal elastica, the integration of the director $\boldsymbol{d_1}$ can be addressed afterward:

$$\dot{\boldsymbol{d_1}} = (\boldsymbol{d_3} \times \dot{\boldsymbol{d_3}}) \times \boldsymbol{d_1} + \frac{m_3}{\gamma} \boldsymbol{d_3} \times \boldsymbol{d_1}. \tag{18}$$

The register symmetry (continuous rotation of the rod material around its centre line) present here as in any isotropic rod, no longer is a source of trouble (non-isolation of solutions) since it is decoupled from the boundary value problem (13), (14), (19) and (20). It just boils down to choosing an initial value for the rotation angle of $\boldsymbol{d_1}(0)$ in the plane $(\boldsymbol{e_y}, \boldsymbol{d_3}(0) \times \boldsymbol{e_y})$.

We note $\boldsymbol{m}(0) = (m_{x0}, m_{y_0}, m_{z0})$ and we will refer to m_{z0} as simply m_z since it does not depend on s. The constant m_3 is given by $m_3 = m_{x0} d_{3x}(0) + m_z d_{3z}(0)$.

2.4. CLAMPED BOUNDARY CONDITIONS

We consider the case where the rod is held in a strong anchoring way: at both side the position and the tangent of the rod are fixed. Moreover in what we call a clamped configuration, the tangent of the rod at both ends is aligned with the axis joining the two ends (see Figure 2). These clamped boundary conditions can be written as

$$\boldsymbol{d_3}(-\pi) = \boldsymbol{d_3}(\pi), \tag{19}$$

$$\boldsymbol{r}(\pi) - \boldsymbol{r}(-\pi) = k\boldsymbol{d_3}(\pi) \quad \text{with } k \in]-2\pi; 2\pi]. \tag{20}$$

We denote (see Figure 2) A_1 and A_2 the two end-points (orienting the arc-length S from A_1 to A_2) and we define the end shortening d as

$$\begin{aligned} d &\stackrel{\text{def}}{=} \frac{D}{L} \stackrel{\text{def}}{=} \frac{L - (\boldsymbol{R}(A_2) - \boldsymbol{R}(A_1)) \cdot \boldsymbol{d_3}(A_2)}{L} \\ &= 1 - \frac{(\boldsymbol{r}(\pi) - \boldsymbol{r}(-\pi)) \cdot \boldsymbol{d_3}(\pi)}{2\pi} = 1 - \frac{k}{2\pi}. \end{aligned} \tag{21}$$

This is the difference of the distance between the ends when the rod is buckled compared to the distance between the ends when the rod is straight ($= L$). Circularly closed configurations (also called rings) have $d = 1$.

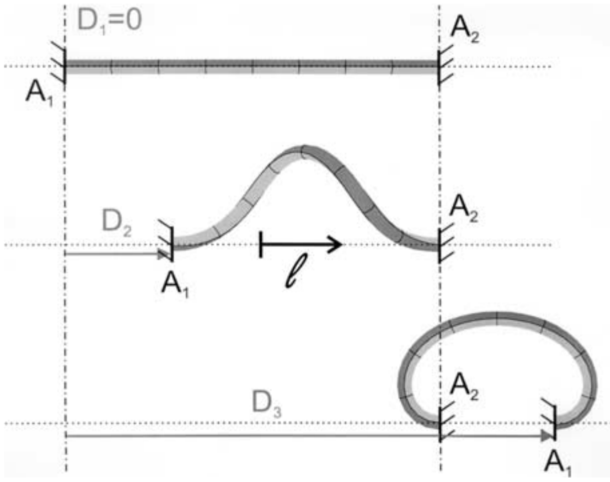

Figure 2. A rod with clamped boundary conditions: the axis $\boldsymbol{\ell}$ (joining point A_1 to point A_2) and the tangent of the rod at both ends are aligned. The end-shortening D_i of a configuration is the distance between the point A_1 in that configuration and the point A_1 in a straight configuration: $D_1 = 0$, $0 < D_2 < L$ and $L < D_3 < 2L$.

The fact that we do not write any condition on $\boldsymbol{d_1}$ at either end does not mean that the solutions of the present boundary value problem are going to be twistless. Indeed once a solution is known for $\boldsymbol{r}(s)$ and $\boldsymbol{d_3}(s)$, the function $\boldsymbol{d_1}(s)$ is imposed by (18) and will not in general yield a twistless rod. We just happen to not compute $\boldsymbol{d_1}(s)$ because we are not interested here with futures like the rotation of $\boldsymbol{d_1}(A_1)$ with regard to $\boldsymbol{d_1}(A_2)$ (also called the *end-rotation*).

3. Reversibility of the Solutions

In this section we show that only solutions with certain symmetries fulfill the clamped boundary conditions. Namely, all clamped solutions have a rotational C_2 symmetry (also called π-flip symmetry). This generalizes [8] where the statement was proved for circularly closed configurations (i.e. rings). Then we show how our choice of parameters (and placing of $s = 0$ at the middle of the rod) yields a natural factorization of the classic cubic polynomial. This subsequently enables us to write the boundary conditions as 2 implicit equations for the 4 parameters of the problem.

3.1. REDUCTION TO AN EQUIVALENT OSCILLATOR

Instead of considering equations (13) and (14) together with integrals of motion (15)–(17), we make use of the integrals of motion to further reduce the system [1, 26]. Introducing Euler spherical angles θ and ψ to parametrize the unit vector $\boldsymbol{d_3}$

$$d_{3x} = \sin\theta\cos\psi, \qquad d_{3y} = \sin\theta\sin\psi, \qquad d_{3z} = \cos\theta, \tag{22}$$

we can re-write the equilibrium equations (13) and (14) as

$$\dot{\theta} = \omega, \qquad \dot{\omega} = -\frac{\mathrm{d}V}{\mathrm{d}\theta}, \tag{23}$$

$$\dot{\psi} = \frac{m_z - m_3 \cos\theta}{\sin^2\theta} \tag{24}$$

with

$$V(\theta) = \frac{(m_z - m_3\cos\theta)^2}{2\sin^2\theta} + f\cos\theta. \tag{25}$$

System (23)–(25) has m_z, m_3, f as parameters and θ_0, ω_0 as initial conditions.

Equations (23) are the equations of an undamped nonlinear oscillator of potential $V(\theta)$, while equation (24) can be integrated afterwards. In order to ensure $d_{3y}(0) = 0$ we will either take $\theta(0) = 0 \bmod \pi$ or $\psi(0) = 0$. In the phase plane (ω, θ) the trajectories are the level curves of the energy function $H(\omega, \theta) = \frac{1}{2}\omega^2 + V(\theta)$ which is precisely the integral of motion $I_2 - \frac{1}{2}m_3^2$ (see equation (17)).

A dynamical system $\dot{\boldsymbol{v}} = \boldsymbol{F}(\boldsymbol{v})$ is reversible in the sense of Devaney [4] if it is invariant under the reversing involution:

$$s \to -s, \qquad \boldsymbol{v} \to \mathbb{P}\boldsymbol{v} \quad \text{with } \mathbb{P}^2 = \mathbb{I} \tag{26}$$

Clearly, system (23) is reversible with

$$s \to -s \qquad \theta \to \theta, \qquad \omega \to -\omega, \tag{27}$$

its phase plane has the following symmetry: trajectories are the same up and down of the θ axis with the arrows of the vector field reversed. The system also has this other reversible symmetry:

$$s \to -s, \qquad \theta \to -\theta, \qquad \omega \to \omega, \tag{28}$$

hence trajectories are the same left and right of the axis $\theta = 0 \bmod \pi$ with the time arrows reversed.

Now a solution of a reversible system will be call a *reversible solution* if it has its initial condition on the invariant set of the symmetry (e.g., the θ axis for symmetry (27)). Such a solution will have odd or even properties for its variables (e.g., the solution in bold in Figure 3 is even in θ and odd in ω).

In the next section we will show that the rotational C_2 symmetry we want to prove for the centre line of the rod is equivalent to having a reversible solution in the phase plane.

As soon as $\theta(s)$ and $\psi(s)$ are known, we can integrate equation (22) to get the centre line $\boldsymbol{r}(s)$. We can then get $\boldsymbol{m}(s)$ by either using equation (9) or using equation (6) together with the relation between Euler angles and $\boldsymbol{u}$ (see, for example, [26]). To each trajectory of the phase space (θ, ω, ψ) is associated a configuration of the rod.

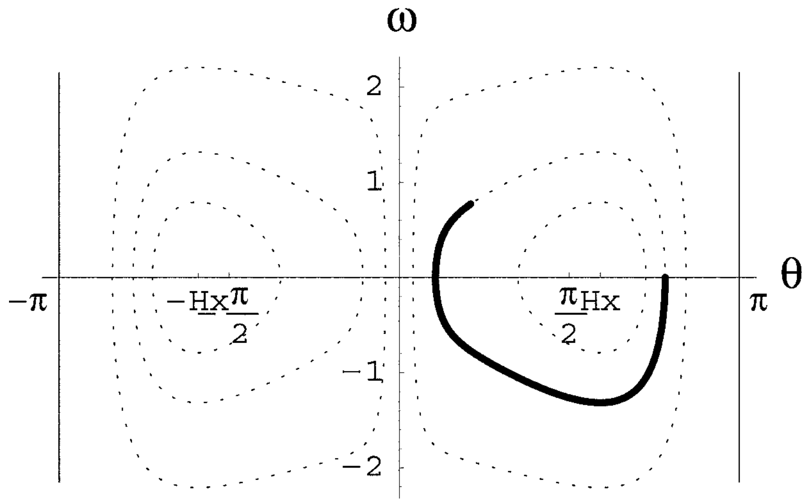

Figure 3. Phase space of the system (23) with $(m_z, m_3, f) = (-0.52257, -0.76464, 0.79883)$. Bold trajectory is with $(\theta(0), \omega(0)) = (2.457, 0)$ (yielding $H = 0.9373$) integrated form $s = 0$ up to $s = +\pi$.

3.2. CLAMPED SOLUTIONS ARE REVERSIBLE

The clamped boundary conditions equation (19) can be written either as

$$\begin{aligned} &\theta(-\pi) = \theta(+\pi) \mod 2\pi \quad \text{and} \\ &\theta(+\pi) = 0 \mod \pi, \end{aligned} \tag{29}$$

or

$$\theta(-\pi) = \theta(+\pi) \mod 2\pi \quad \text{and} \tag{30}$$

$$\theta(+\pi) \neq 0 \mod \pi \quad \text{and}$$

$$\psi(-\pi) = \psi(+\pi) \mod 2\pi, \tag{31}$$

or

$$\theta(-\pi) = -\theta(+\pi) \mod 2\pi \quad \text{and} \tag{32}$$

$$\theta(+\pi) \neq 0 \mod \pi \quad \text{and}$$

$$\psi(-\pi) = \pi + \psi(+\pi) \mod 2\pi. \tag{33}$$

LEMMA. *These clamped boudary conditions implies that the solutions of the system* (23)–(25) *are reversible with either*

$$\theta(-s) = \theta(s), \qquad \omega(-s) = -\omega(s), \qquad \psi(-s) = -\psi(s) \tag{34}$$

or

$$\theta(-s) = -\theta(s), \qquad \omega(-s) = \omega(s), \tag{35}$$

$$\psi(-s) = \pi - \psi(s) \qquad (\textit{or respectively } \psi(-s) = -\pi - \psi(s)). \tag{36}$$

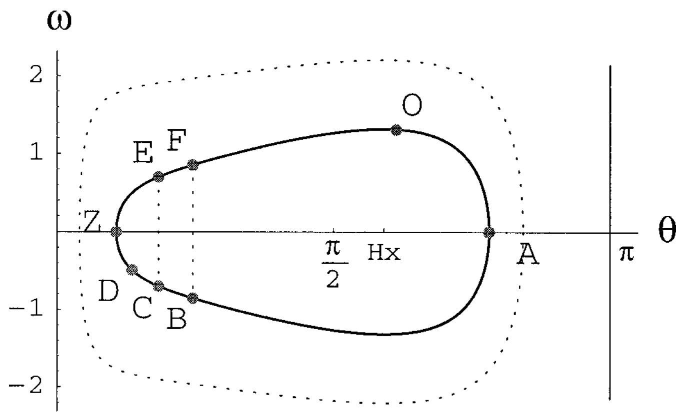

Figure 4. The trajectory $H = 0.9373$ and different possibilities of choosing the initials conditions $(\theta(0), \omega(0))$.

Proof. The (generic) case $m_z \neq \pm m_3$. A typical phase plane with $m_z \neq \pm m_3$ is shown in Figure 3, where trajectories are turning around the point H_X (corresponding to a helical centre line) in a clockwise way. In this case where $\theta(0) = 0 \bmod \pi$ is not possible, we take $\psi(0) = 0$ in order to have $d_{3y}(0) = 0$. In Figure 4, we consider a trajectory which evolves on a certain level set of $H = H(\omega, \theta)$, with period $T = T(H)$. We choose an initial condition with $\omega \neq 0$ at point O. From that point where $s = 0$, we have to integrate back (down to $s = -\pi$) and forth (up to $s = +\pi$) to reach the ends of the rod. Let us call B the point where $s = -\epsilon\pi$ and D the point where $s = +\epsilon\pi$ (with $\epsilon = \pm 1$). The point C is such that $s(C) = T/2$. Equations (32) or (29) cannot be fulfilled in this case, so we only consider equation (30) which implies that the two points B and D must have the same value for θ. Two cases have to be considered:

Case α. The trajectory under consideration has exactly a period $T = 2\pi$ (or a sub-multiple of it $nT = 2\pi$ with $n > 1$), so points B, C and D coincide. Such solutions that in addition fulfil boundary conditions (31) correspond to configurations with a periodic centre line, i.e. circularly closed rods. To show this, we write the $\boldsymbol{e_x}$ and $\boldsymbol{e_y}$ components of $\boldsymbol{m}$ using equations (9) and (11):

$$fx + m_{y0} = m_y = \frac{m_3 - m_z \cos\theta}{\sin\theta} \sin\psi + \omega \cos\psi, \tag{37}$$

$$-fy + m_{x0} = m_x = \frac{m_3 - m_z \cos\theta}{\sin\theta} \cos\psi - \omega \sin\psi. \tag{38}$$

Let us now calculate $\boldsymbol{r}(\pi) - \boldsymbol{r}(-\pi)$ when the solution fulfils boundary conditions (30) and (31). Using (37) and (38) we have

$$x(\pi) - x(-\pi) = x_D - x_B = \frac{1}{f}(\omega_D - \omega_B) \cos\psi_D, \tag{39}$$

$$y(\pi) - y(-\pi) = y_D - y_B = \frac{1}{f}(\omega_D - \omega_B)\sin\psi_D. \tag{40}$$

Since B and D coincide, $\omega_D = \omega_B$ and then the differences are vanishing: $x_D = x_B$ and $y_D = y_B$. Now the other boundary condition (20) implies that either $k = 0$ or $(d_{3z}(\pi) = \pm 1 \Leftrightarrow \theta_D = 0 \bmod \pi)$. The latter case being only possible when $m_3 = \pm m_z$ and corresponding to a point O on the ω axis (see further down). The property $k = 0$ means $\boldsymbol{r}(\pi) = \boldsymbol{r}(-\pi)$, i.e., a closed rod. Then, making use of the translational invariance in arc-length of such configurations, we can shift the origin of arc-length in order to bring point O either on Z or A. In fact in continuation procedures, we will only consider closed solutions starting at Z or A as this locally isolate the solutions (in the parameter space), solving the degeneracy problem due to the translation invariance of arc-length in rings. See [17] for a detailed discussion about this continuous symmetry.

REMARK. An example of closed rods solutions with $\omega(0) \neq 0$ is the connection (explained in [6]) between the first (respectively any p odd) and the second (respectively and the even $p + 1$) inflexional planar elastica. Along this connection, the starting point O and the ending point C are turning around the trajectory and eventually invert their mutual positions.

Case β. Point D has to coincide with point F, due to equation (30). But since $s_{B\to C}$ is equal to $s_{C\to D}$, we have $s_{B\to C} = s_{C\to F}$. Now $s_{C\to F} = s_{C\to E} + s_{E\to F}$ and reversibility (27) implies that $s_{B\to C} = s_{E\to F}$. So we must have $s_{C\to E} = 0$, i.e. C, E and Z coinciding. From the definition of point C, this implies that the point O has to coincide with point A, i.e., being on the (invariant) axis θ with $\omega(0) = 0$. Hence the solution functions are themselves reversible, i.e., either odd or even, obeying (34). Using the relation between Euler angles and $\boldsymbol{u}$ (see, for example, [26]) and equation (6) we have

$$\begin{aligned} \boldsymbol{m}(0)\cdot\boldsymbol{e_y} &= m_1(0)d_{1y}(0) + m_2(0)d_{2y}(0) + m_3 d_{3y}(0) \\ &= -\dot{\psi}(0)\sin\theta(0)\sin\psi(0)\cos\theta(0) + \omega(0)\cos\psi(0) \\ &\quad + m_3\sin\psi(0)\sin\theta(0). \end{aligned} \tag{41}$$

Remember that we took $\psi(0) = 0$ to have $d_{3y}(0) = 0$. This together with $\omega(0) = 0$ yields $m_{y0} = 0$.

The case $m_z = \pm m_3 \neq 0$. In this case the phase plane topology is different and some extra care must be taken since equations (32) or (29) can now be fulfilled.

$f \leqslant 4m_z^2$. A typical phase plane is shown in Figure 5.

If we consider the boundary equation (30), the same arguments as in the former case $m_z \neq \pm m_3$ can be applied to show that either point O has to be choosen on

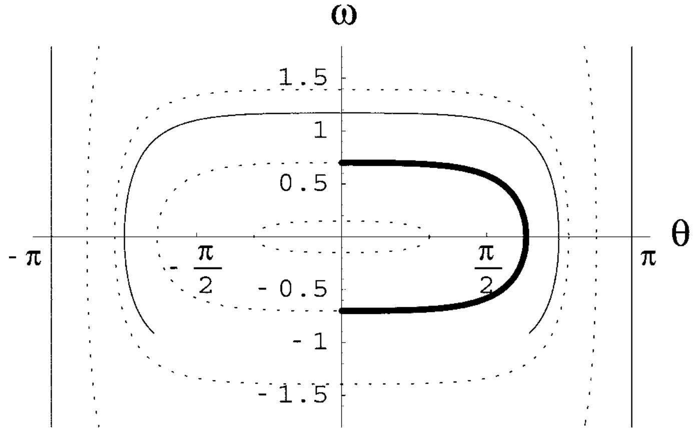

Figure 5. Phase plane for the case $m_z = +m_3 \neq 0$ with $f \leqslant 4m_z^2$. The diagram would be shifted horizontally of π in the case $m_z = -m_3 \neq 0$.

the θ axis (case β), leading to reversible solutions with the property (34), or that the trajectory is closed (case α) which in turn implies a closed rod configuration.

If we consider the boundary equation (32), the arguments of case β forces the point O to be on the ω axis (or the line $\theta = \pi \mod 2\pi$). This corresponds to the trajectory drawn plain line in Figure 5.

If we consider the boundary equation (29), the symmetry (28) forces the point O to be on the ω axis (or the line $\theta = \pi \mod 2\pi$). This corresponds to the bolded half trajectory in Figure 5.

In these two latter cases we have nevertheless a reversible solution, obeying (35).

$f > 4m_z^2$. Here the phase plane contains an homoclinic trajectory. The arguments of case $m_z \neq \pm m_3$ can be fully applied to the trajectories inside the homoclinic curve (which itself can fulfill the boundary condition (29)). As for the trajectories around the homoclinic curve, the discussion is the same as in the case $f \leqslant 4m_z^2$, leading to the possibilities of trajectories having the point O on the ω axis (or the line $\theta = \pi \mod 2\pi$), which implies reversibility (35) for the solutions, see Figure 6.

All the cases where point O is taken on the ω axis (or respectively on the line $\theta = \pi \mod 2\pi$) have the property $d_{3y}(0) = 0$ without needing $\psi(0) = 0$. We choose $\psi(0) = \pi/2$ (or respectively $\psi(0) = -\pi/2$) in order to have (36). This will ensure the same symmetries for the centre line (42) and (43) as in the case $m_z \neq \pm m_3$. With $\psi(0) = \pm\pi/2$ and $\theta(0) = 0 \mod \pi$, equation (41) shows that here also $m_{y0} = 0$.

The case $m_z = m_3 = 0$. This case is well known and it is rather easy to check that solutions fulfilling clamped boundary conditions either start on the θ axis or on the ω axis which are invariant axis of the symmetries (27) or (28), respectively.

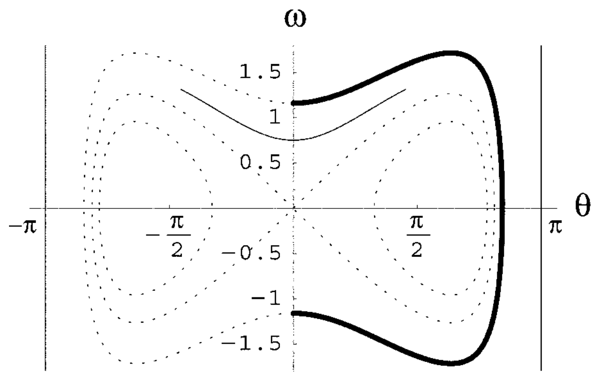

Figure 6. Phase plane for the case $m_z = +m_3 \neq 0$ with $f > 4m_z^2$. The diagram would be shifted horizontally of π in the case $m_z = -m_3 \neq 0$.

This in turn implies that the centre line (which live in 2D) has the symetries (42) and (43).

In conclusion, in all three cases $\{m_z \neq \pm m_3, m_z = \pm m_3 \neq 0, m_z = \pm m_3 = 0\}$ we have reversibility of the solutions (equation (34) or equation (35) together with equation (36)). □

THEOREM. *All the clamped configurations of the ideal elastica have the following symmetries:*

$$x(-s) = -x(s), \qquad y(-s) = y(s), \qquad z(-s) = -z(s), \tag{42}$$

$$d_{3x}(-s) = d_{3x}(s), \qquad d_{3y}(-s) = -d_{3y}(s), \qquad d_{3z}(-s) = d_{3z}(s), \tag{43}$$

$$m_x(-s) = m_x(s), \qquad m_y(-s) = -m_y(s). \tag{44}$$

Proof. Starting from the symmetry properties (34)–(36), one get property (43) by considering (22). Then integrating (43) with the fact that $d_{3y}(0) = 0$ yields (42). Finally, (44) comes from (9) and the fact that in all cases we can choose $m_y(0) = 0$ without loss of generality. □

This symmetry has been studied in [8] where it is refered as π-flip symmetry (C_2 rotational symmetry about our y axis). There the theorem was proven for circularly closed configurations (i.e., rings), a special case of our clamped solutions. Nevertheless shear and extensibility where included in the model of [8]. This flip symmetry happens in fact as soon as, at a certain point along the rod (which for us is $s = 0$), the three vectors $\boldsymbol{d_3}$, $\boldsymbol{f}$ and $\boldsymbol{m}$ lie in the same plane.

3.3. BOUNDARY CONDITIONS AS IMPLICIT EQUATIONS FOR THE PARAMETERS

Considering the cases $m_z = \pm m_3 \neq 0$ and $m_z = \pm m_3 = 0$ as marginal cases, we will from now on start integration at point A or Z and call θ_0 the value of $\theta(s)$ at the starting point. Hence we have $d_{3x}(0) = \sin\theta_0$, $d_{3y}(0) = 0$, $d_{3z}(0) = \cos\theta_0$ and

$$m_3 = m_z \cos\theta_0 + m_{x0} \sin\theta_0 \tag{45}$$

and

$$H = \frac{1}{2}(m_z \sin\theta_0 - m_{x0}\cos\theta_0)^2 + f\cos\theta_0. \tag{46}$$

It has been shown in [15] and in [22] that solutions of equations (23) and (24) and of the centre line $\boldsymbol{r}$ can be expressed in term of elliptic functions. This scheme is used in [24, 3]. Nevertheless this involves integration constants that are difficultly related to physical parameters (tension f or twist m_3) or integral of motion m_z. On the other hand, in [21] solutions are written in term of the integrals of motion m_3, m_z, f, H. Following this, we introduce the variable $u \overset{\text{def}}{=} \cos\theta$. Equation (23) is then equivalent to

$$\dot{u}^2 = P_3(u), \tag{47}$$

where

$$P_3(u) \overset{\text{def}}{=} 2(H - fu)(1 - u^2) - (m_z - m_3 u)^2. \tag{48}$$

Since m_3 takes the same value for different values of m_z, θ_0 and m_{x0}, we will not use it. Using m_{x0} and $u_0 \overset{\text{def}}{=} \cos\theta_0$ instead, we have

$$P_3(u) = (u - u_0)P_2(u) \tag{49}$$

with

$$P_2(u) = 2fu^2 - u(m_z^2 + m_{x0}^2) - 2f + u_0(m_z^2 - m_{x0}^2) + 2m_z m_{x0}\sin\theta_0. \tag{50}$$

To know whether the roots of $P_2(u)$ are real or not, we compute its discriminant Δ:

$$\Delta \overset{\text{def}}{=} (m_z^2 + m_{x0}^2)^2 + 8f(2f + u_0(m_{x0}^2 - m_z^2)) - 16 m_z m_{x0} f \sin\theta_0. \tag{51}$$

Considering Δ as a second degree polynomial in f and calculating its own discriminant, we see this Δ is always positive, i.e., the two roots of $P_2(u)$ are real. Evaluating $P_2(u = 1) = (m_z - m_3)^2/(u_0 - 1) \leqslant 0$ and keeping in mind that we only consider strictly positive f we see that there always is a root $u_+ \geqslant 1$. Evaluating $P_2(u = -1) = (m_z + m_3)^2/(u_0 + 1) \geqslant 0$, we see that the other root $u_- \in [-1, 1]$,

$$u_+ = \frac{1}{4f}\left(m_z^2 + m_{x0}^2 + \sqrt{\Delta}\right), \qquad u_- = \frac{1}{4f}\left(m_z^2 + m_{x0}^2 - \sqrt{\Delta}\right). \tag{52}$$

Now in order to express $\theta(s)$, $\psi(s)$ in term of elliptic functions, we need to know whether u_0 is greater or less than u_-. This is given by the sign of

$$P_2(u_0) = -2f - 2u_0 m_{x0}^2 + 2fu_0^2 + 2m_z m_{x0}\sin\theta_0, \tag{53}$$

with $P_2(u_0)$ negative corresponding to $u_0 > u_-$. We call the solution an *odd harmonic* when $u_0 < u_-$ and an *even harmonic* when $u_0 > u_-$ and we define:

$$\mu_\pm \stackrel{\text{def}}{=} \mp \frac{|u_0 - u_-|}{1 \pm \min(u_0, u_-)}, \qquad \nu \stackrel{\text{def}}{=} u_+ - \min(u_0, u_-) \geqslant 0,$$
$$m \stackrel{\text{def}}{=} \frac{|u_0 - u_-|}{\nu} \leqslant 1. \tag{54}$$

In the *odd harmonic* case, equation (47) is integrated as

$$u(s) = \cos\theta(s) = u_0 + (u_- - u_0)\sin^2(\bar{s}) \tag{55}$$

and equation (24) is integrated as

$$\psi(s) = \sqrt{\frac{1}{2f\nu}}\left\{\left(m_z + m_{x0}\frac{\sin\theta_0}{1+u_0}\right)\Pi(\mu_+, \bar{s}, m) + \left(m_z - m_{x0}\frac{\sin\theta_0}{1-u_0}\right)\Pi(\mu_-, \bar{s}, m)\right\}, \tag{56}$$

where $\bar{s} = \text{ am }(s\sqrt{f\nu/2}, m)$. As for the centre line, $x(s)$ and $y(s)$ can be extracted from (37) and (38). The coordinate $z(s)$ is obtained by integrating (55):

$$z(s) = u_+ s - \sqrt{\frac{2\nu}{f}} E(\bar{s}, m) \quad \text{with } \nu = u_+ - u_0. \tag{57}$$

In the *even harmonic* case, we find:

$$u(s) = \cos\theta(s) = u_- + (u_0 - u_-)\sin^2(\hat{s}), \tag{58}$$

$$\psi(s) = \sqrt{\frac{1}{2f\nu}}\left\{\frac{m_z(1+u_0) + m_{x0}\sin\theta_0}{1+u_-}\big(\Pi(\mu_+, \hat{s}, m) - \overline{\Pi}(\mu_+, m)\big) + \frac{m_z(1-u_0) - m_{x0}\sin\theta_0}{1-u_-}\big(\Pi(\mu_-, \hat{s}, m) - \overline{\Pi}(\mu_-, m)\big)\right\}, \tag{59}$$

$$z(s) = u_+ s - \sqrt{\frac{2\nu}{f}}\big(E(\hat{s}, m) - \overline{E}(m)\big) \quad \text{with } \nu = u_+ - u_- = \frac{\sqrt{\Delta}}{2f}, \tag{60}$$

where $\hat{s} = \text{am}(s\sqrt{f\nu/2} + K(m), m)$.

In both cases the solution $\theta(s)$ has the period

$$T = 2\sqrt{2}\frac{K(m)}{\sqrt{f\nu}}. \tag{61}$$

Using (34) the boundary condition (31) reduces to

$$\psi(\pi) = 0 \mod \pi. \tag{62}$$

Using the symmetries (42) and (43), equation (20) reduces to

$$x(\pi)d_{3z}(\pi) - z(\pi)d_{3x}(\pi) = 0. \tag{63}$$

Then putting (62) in (37) we get $fx(\pi) = \omega(\pi)$ and since $\theta(\pi) \neq 0$, we can write the second boundary condition as

$$u'(\pi)u(\pi) + f\big(1 - u^2(\pi)\big)z(\pi) = 0. \tag{64}$$

This can in turn be written in terms of the parameters $(f, m_z, m_{x0}, \theta_0)$.

Using equations (55)–(57) for the *odd harmonic* case:

$$\sqrt{\frac{1}{2f\nu}}\left\{\left(m_z + m_{x0}\frac{\sin\theta_0}{1+u_0}\right)\Pi(\mu_+, \bar{s}_\pi, m) + \left(m_z - m_{x0}\frac{\sin\theta_0}{1-u_0}\right)\Pi(\mu_-, \bar{s}_\pi, m)\right\} = 0 \mod \pi, \tag{65}$$

$$\sqrt{2f\nu}\big(u_0 + (u_- - u_0)\sin^2(\bar{s}_\pi)\big)(u_- u_0)\sin\bar{s}_\pi\cos\bar{s}_\pi\sqrt{1 - m\sin^2\bar{s}_\pi} + f\big(1 - (u_0 + (u_- - u_0)\sin^2\bar{s}_\pi)^2\big)\left(u_+\pi - \sqrt{\frac{2\nu}{f}}E\big(\bar{s}_\pi, m\big)\right) = 0, \tag{66}$$

with $\bar{s}_\pi = \mathrm{am}(\pi\sqrt{f\nu/2}, m)$.

And using equations (58)–(60) for the *even harmonic* case:

$$\sqrt{\frac{1}{2f\nu}}\left\{\frac{m_z(1+u_0) + m_{x0}\sin\theta_0}{1+u_-}\big(\Pi(\mu_+, \hat{s}_\pi, m) - \overline{\Pi}(\mu_+, m)\big) + \frac{m_z(1-u_0) - m_{x0}\sin\theta_0}{1-u_-}\big(\Pi(\mu_-, \hat{s}_\pi, m) - \overline{\Pi}(\mu_-, m)\big)\right\} = 0 \mod \pi, \tag{67}$$

$$\sqrt{2f\nu}\big(u_- + (u_0 - u_-)\sin^2(\hat{s}_\pi)\big)(u_0 - u_-)\sin\hat{s}_\pi\cos\hat{s}_\pi\sqrt{1 - m\sin^2\hat{s}_\pi} + f\big(1 - \big(u_- + (u_0 - u_-)\sin^2\hat{s}_\pi\big)^2\big) \times \left(u_+\pi - \sqrt{\frac{2\nu}{f}}(E(\hat{s}_\pi, m) - E(m))\right) = 0, \tag{68}$$

with $\hat{s}_\pi = \mathrm{am}(\pi\sqrt{f\nu/2} + K(m), m)$.

The case of the homoclinic trajectory $\theta(\pi) = 0$ and $\omega(\pi) = 0$ and the case where $\theta(\pi) = 0 \mod \pi$ are limiting cases of these equations.

When actually computing the solution manifold, we are not going to use these equations but we will rather integrate numerically equations (13) and (14) with $m_{y0} = 0$ and use (63) together with

$$d_{3y}(\pi) = 0 \tag{69}$$

(from equations (42), (43), (19)) as boundary conditions.

3.4. CLOSED TRAJECTORIES CORRESPOND TO RINGS OR PLANAR ELASTICAE

In the subcase α of the (generic) case $m_z \neq \pm m_3$, we have seen that under clamped boundary conditions a trajectory in the phase space is closed if and only if the associated rod shape is closed.

Still in the case where $m_z = \pm m_3 \neq 0$, we have seen that closed trajectories starting and ending on the ω axis (or the line $\theta = \pi \mod 2\pi$) may also exist since they fulfill the boundary condition (29) (or (19)): we have $\boldsymbol{d_3}(-\pi) = \boldsymbol{d_3}(\pi) = (0, 0, \pm 1)^{\mathrm{T}}$. Then the other boundary condition (20) requires that $x(-\pi) = x(\pi)$ and $y(-\pi) = y(\pi)$.

Let us see if this is possible, restricting to $m_z = -m_3 \neq 0$, i.e. $\theta(0) = \theta(\pi) = \theta(-\pi) = \pi$. We recall equations (37) and (38), which here read:

$$fx + m_{y0} = m_y \;=\; m_z \mathrm{cotan}\frac{\theta}{2}\sin\psi + \omega\cos\psi, \tag{70}$$

$$-fy + m_{x0} = m_x \;=\; m_z \mathrm{cotan}\frac{\theta}{2}\cos\psi - \omega\sin\psi. \tag{71}$$

Then using (36) we get:

$$x(\pi) - x(-\pi) \;=\; \frac{1}{f}\big(\omega(\pi) + \omega(-\pi)\big)\cos\psi(\pi), \tag{72}$$

$$y(\pi) - y(-\pi) \;=\; \frac{1}{f}\big(\omega(\pi) - \omega(-\pi)\big)\sin\psi(\pi). \tag{73}$$

By symmetry of the phase plane, $\omega(\pi) = \omega(-\pi)$, hence $y(\pi) = y(-\pi)$. But we need $\psi(\pi) = \pi/2 \mod \pi$ in order to secure $x(\pi) = x(-\pi)$. Here $\psi(s)$ can be integrated to give:

$$\psi(s) = \sqrt{\frac{1}{2f\nu}}\, m_z \Pi(\mu_-, \bar{s}(s), m) - \frac{\pi}{2}$$
$$\text{with } \nu = u_+ + 1,\; \mu_- = \frac{u_- + 1}{2},\; m = \frac{2\mu_-}{\nu}. \tag{74}$$

In order that $\theta(\pi) = \theta(0) = \pi$, we need (from (55)) $\bar{s}(\pi) = \pi$. Considering $\psi(\pi)$ as a function of the 3 variables (m_z, m_{x0}, f) it can then be verified that $\psi(\pi) \in [-3\pi/2; \pi/2]\forall(m_z, m_{x0}, f)$, the two limits being reached when either $m_z = 0$ or $f = 0$. The solutions with $m_z = 0$ that have $\bar{s}(\pi) = \pi$ are planar elastica. The ones with $f = 0$ are untiwsted rings.

In conclusion we state that under clamped boundary conditions a trajectory in the phase space is closed if and only if the associated rod shape is closed or planar.

4. Classification of the Clamped Configurations

In this section we provide a classification of the clamped configurations using the pulsation of their associated trajectories in the phase plane and we assign them a label. Equivalently the classification is done by counting the number of points of maximum and minimum curvature along the centre line. We show that the circularly closed configurations are separating the sets of configurations with different labels.

4.1. DEFINITION OF AN HARMONIC

Consider a solution of (23) and (24) that fulfills boundary condition (29) or (30)–(31) or (32)–(33). We define the pulsation

$$\Omega \stackrel{\text{def}}{=} \frac{2\pi}{T} \tag{75}$$

and the (integer) label n:

$$\text{(odd)} \quad n \stackrel{\text{def}}{=} 1 + 2\,\mathrm{Int}\left(\frac{\Omega - 1}{2}\right) \quad \text{if } u_- > u_0, \tag{76}$$

$$\text{(even)} \quad n \stackrel{\text{def}}{=} 2 + 2\,\mathrm{Int}\left(\frac{\Omega - 1}{2}\right) \quad \text{if } u_- < u_0, \tag{77}$$

where u_- is given by equation (52), $u_0 = \cos\theta_0$ and $\mathrm{Int}(x) = i$ such that $i \leqslant x < i + 1$. The label n is completed by a sign $\pm$ which is the sign of k in equation (20) (this is also the sign of $d - 1$, see equation (21)). We will refer to a solution as to a $n^{\pm}$ *harmonic*. The case $u_- = u_0$ corresponds to planar rings for which n is in between two following integers and $k = 0$. Other $k = 0$ solutions are buckled rings where n is not defined.

4.2. SPECIAL SOLUTIONS

Here we list some special solutions and give their Ω value:

Planar (untwisted) elastica. The planar elastica solutions are defined by

$$I_0 = 0 \quad \text{and} \quad I_1 = 0. \tag{78}$$

They are divided into two families: inflexional and non-inflexional [18]. With $f > 0$, (78) implies that $m_z = 0$.

The pth non-inflexional planar elastica have ${m_{x0}}^2 > 4f$:

$$\begin{aligned} \theta_0 = 0 \quad &\Rightarrow \quad u_+ = \frac{m_{x0}^2}{2f} + 1 > u_0 = 1 > u_- = -1 \\ &\Rightarrow \quad m = \left(1 + \frac{m_{x0}^2}{4f}\right)^{-1}, \quad \nu = \frac{m_{x0}^2}{2f} + 2, \end{aligned} \tag{79}$$

$$\begin{aligned} \theta_0 = \pi \quad &\Rightarrow \quad u_+ = \frac{m_{x0}^2}{2f} - 1 > u_- = 1 > u_0 = -1 \\ &\Rightarrow \quad m = \frac{4f}{m_{x0}^2}, \quad \nu = \frac{m_{x0}^2}{2f}, \end{aligned} \tag{80}$$

where $K(m)$ is the complete elliptic integral of the first kind (see Appendix). In both cases boundary conditions imply that $\Omega = p$.

The pth (p odd) inflexional planar elastica has ${m_{x0}}^2 < 4f$:

$$\theta_0 = \pi \quad \Rightarrow \quad u_+ = 1 > u_- = \frac{m_{x0}^2}{2f} - 1 > u_0 = -1$$
$$\Rightarrow \quad m = \frac{m_{x0}^2}{4f}, \quad \nu = 2. \tag{81}$$

Boundary conditions imply that $\Omega = p + 1$.

The pth (p even) inflexional planar elastica has θ_0 that span in $]0; \pi]$ or $[\pi; 2\pi[$ and

$$m_{x0} = 0 \quad \Rightarrow \quad u_+ = 1 > u_0 = \cos\theta_0 > u_- = -1$$
$$\Rightarrow \quad m = \frac{\cos\theta_0 + 1}{2}, \quad \nu = 2. \tag{82}$$

Boundary conditions imply that $\Omega \in [2\sqrt{f_b}, p - 1]$, where f_b is the pth solution of $\tan \pi\sqrt{f} = \pi\sqrt{f}$.

Planar rings (twisted or not). Planar rings correspond to a helix ($u_- = u_0$) of null pitch angle ($\theta(s) \equiv \theta_0 = \pi/2 \bmod \pi$). This implies

$$u_- = u_0 = 0 \quad \Rightarrow \quad m = 0, \quad \sqrt{\Delta} = m_z^2 + {m_{x0}}^2$$
$$\Rightarrow \quad \nu = u_+ = \frac{\sqrt{\Delta}}{2f}, \quad \Omega = \Delta^{1/4}. \tag{83}$$

The twisting moment $m_3 = \pm m_{x0}$ rises with Ω.

Buckled rings. Closed configurations have closed trajectories in the phase plane. Hence they have integer Ω.

4.3. TRAJECTORIES EXTREMA, CURVATURE AND XY PROJECTION

The radial deflection (the projection of the centre line on a plane perpendicular to the force vector) of any unshearable rod always evolves between two circles (see [13]). Here we explain that, in the case of the ideal elastica, the extrema of the radial deflection are related to the extrema of the curvature of the centre line and to the points A and Z in the (θ, ω) phase plane. The curvature of the centre line of the rod is defined as:

$$\kappa^2(s) = \boldsymbol{u}_\perp^2(s) = \dot{\boldsymbol{d}}_{\boldsymbol{3}}^2. \tag{84}$$

Using equations (22), (24) and (25) we have

$$\kappa^2(s) = 2(H - f\cos\theta(s)). \tag{85}$$

Since $\theta(s)$ evolves between u_0 and u_-, the curvature is bounded by the two extrema $2(H - fu_0)$ and $2(H - fu_-)$. Writing the moment $\boldsymbol{m}(s)$ in two different ways, on the one hand, using equations (6) and (10),

$$\boldsymbol{m}(s)^2 = \boldsymbol{u}_\perp(s)^2 + \gamma \boldsymbol{u}_\parallel{}^2 = \kappa^2(s) + m_3{}^2, \tag{86}$$

and on the other hand, using equation (9),

$$\boldsymbol{m}(s)^2 = f^2\left(\left(y(s) - \frac{m_{x0}}{f}\right)^2 + x(s)^2\right) + m_z^2, \tag{87}$$

we see that the curvature is also given by

$$\kappa^2(s) = f^2\left(\left(y(s) - \frac{m_{x0}}{f}\right)^2 + x(s)^2\right) + m_z^2 - m_3^2. \tag{88}$$

Using this and equation (85), we write the projection of the centre line on the XY plane as

$$\begin{aligned}\left(y(s) - \frac{m_{x0}}{f}\right)^2 + x(s)^2 &= \frac{1}{f^2}\left\{2(H - f\cos\theta(s)) - m_z^2 + m_3^2\right\}\\ &= \frac{1}{f^2}\left\{\kappa^2(s) - m_z^2 + m_3^2\right\}.\end{aligned} \tag{89}$$

This projection evolves between two circles of radii R_0 and R_- and centre $(0, m_{x0}/f)$ with

$$R_0 = \frac{m_{x0}}{f} \quad \text{and} \quad R_-^2 = \frac{1}{f^2}\left(2(H - fu_-) - m_z^2 + m_3^2\right). \tag{90}$$

Equation (89) gives the relation between curvature, radial deflection and the trajectory in the phase plane. The curvature is minimum (respectively maximum) when the projection touches the smallest (respectively largest) circle (see also [24]) and for an odd harmonic (the statement is reversed for an even harmonic), the curvature is minimum (respectively maximum) when in the phase plane the trajectory passes by $\{\theta(s), \omega(s)\} = \{\theta_-, 0\}$ (respectively $\{\theta(s), \omega(s)\} = \{\theta_0, 0\}$), with $u_- = \cos\theta_-$. We have $R_0 > R_-$ for the odd harmonics and $R_0 < R_-$ for the even harmonics.

When $u_0 \neq u_-$, during one period T in the phase plane (θ, ω) the trajectory passes by one point of maximum θ and one point of minimum θ (points A and Z in Figure 4). Using the fact that the integration is made over a range of 2π for s we can deduce the number n_m (respectively n_M) of points of minimum (respectively maximum) curvature there are along a $n^\pm$ harmonic: for example closed configurations have their trajectories winding Ω times in the phase plane, i.e., have Ω points of minimum curvature and Ω points of maximum curvature (see Table I).

The property that opened clamped solutions have their starting point at $\omega(0) = 0$ can be rephrased this way: under clamped boundary conditions, a closed buckled configuration can only be opened at points of maximum or minimum curvature. In-

Table I. Numbers n_m (respectively n_M) of points of minimum (respectively maximum) curvature along the rod centre line for an harmonic n

Harmonic	n^-	n^+_{odd}	n^+_{even}	$n^=$
n_m	$n+1$	$n+1$	$n-1$	Ω
n_M	n	$n+2$	n	Ω

deed, buckled rings have Ω points of minimum curvature and Ω points of maximum curvature and if one where to open it at a regular point, the opened configuration would still have Ω points of minimum curvature and Ω points of maximum curvature, which is impossible (see Table I). The mechanism of opening a closed $n_M = n_m = \Omega$ configuration at (say) a point of maximum curvature either splits it in two points of maximum curvature $n_M = \Omega + 1$ or makes this point vanish $n_M = \Omega - 1$. The newly opened configuration has $n_m = \Omega$ and either $n_M = \Omega - 1$ (and is a n^-) or $n_M = \Omega + 1$ (and is a n^+).

Remark: The definition of the harmonics n is made using Ω, u_- and u_0. Instead we could have used the numbers n_m and n_M of point of maximum and minimum curvature along the rod to define the harmonics. But we believe that extrema of the radial deflection is the property to use (since it is always valid) to classify clamped rods with non symmetrical cross section [11], because in that case the curvature-radial deflection relation no longer holds, neither does the reduction to the equivalent oscillator and the related use of Ω.

4.4. HOMOTOPIES BETWEEN SOLUTIONS

Now that we have seen what is Ω for different special solutions, we would like to know whether there is an homotopy between any two solutions with different values of the label $n^\pm$. From equations (76) and (77) we see that there are two ways to change the label $n^\pm$:

- A first way to change the label $n^\pm$ is when u_- and u_0 change their relative ordering without changing Ω. Clamped configurations where $u_- = u_0$ are planar rings (twisted or not) (see section 4.2) and by crossing these planar rings one can go from $n_1^\pm$ to $n_2^\mp$ (with $n_1 = 2j - 1$ and $n_2 = 2j$ and j a strictly positive integer), exchanging n_M and n_m.
- Another way to change the label $n^\pm$ is to keep the relative ordering of u_- and u_0 while either (A) changing the sign of $d - 1$ or (B) making Ω cross an odd integer.
  Case (A): this means that we pass through a closed configuration.
  Case (B): If Ω is to be an integer, the trajectory in the phase space has to be closed. In section 3.4 we have seen that (under clamped boundary conditions) a closed trajectory in the phase plane $\{\theta, \omega\}$ corresponds to either a circularly closed configuration (where $d = 1$) or a planar elastica. Nevertheless, while

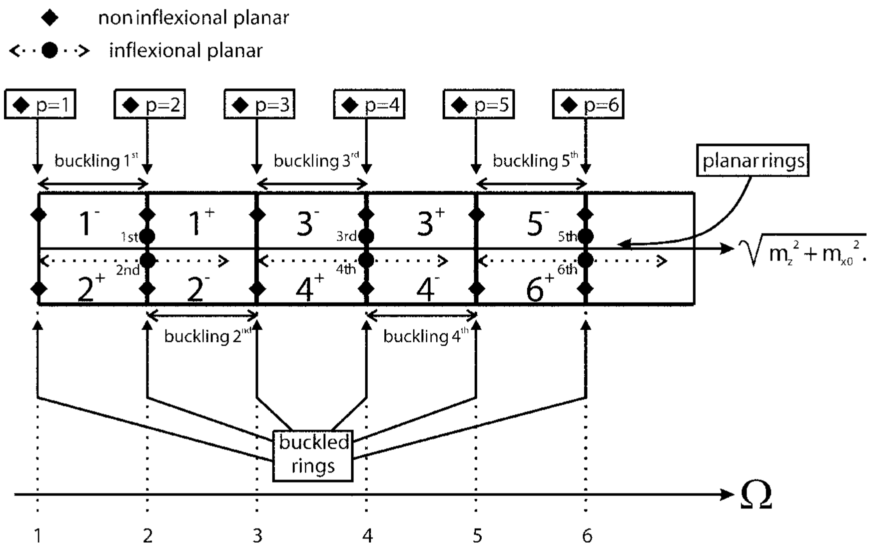

Figure 7. Sketch of the disposition of the different harmonics in the parameter space together with important special solutions (planar or closed). The harmonics are sorted according to their value of $\Omega = \sqrt{m_z^2 + m_{x0}^2}$. The borders that part the different harmonics are the buckled rings that appear for integer value of Ω and the twisted planar rings that exist for continuous value of Ω. All planar configurations but even inflexional one have an integer Ω. Above (respectively under) the line of planar rings, $u_- > u_0$ (respectively $u_- < u_0$) and $u_- = u_0$ on the line.

crossing a planar elastica solution, either m_z changes sign ($\theta_0 = 0 \mod \pi$ and m_{x0} stay unchanged) or both m_z and m_{x0} change sign (θ_0 stays unchanged). Then, due to symmetries of (52), Ω is going to bounce against (and not cross) an integer value. Hence the only possibility in this case (B) to see Ω cross an integer value is to pass through a circularly closed configuration.

Summarizing, we state that changing the label $n^{\pm}$ can only be achieved by crossing a circularly closed configuration (planar or not), i.e., where $d = 1$. In particular this harmonic number $n^{\pm}$ does not change when one rotates the ends about the $\boldsymbol{\ell}$ axis.

4.5. DEALING WITH CONTINUOUS SYMMETRIES

In boundary value problems, continuous symmetries create difficulties for numerical continuation in the sense that numerical continuation requires the Jacobian to be of full rank, and the presence of continuous symmetries violates this condition. Let us consider an equilibrium configuration $(\boldsymbol{r}(s), \boldsymbol{d_1}(s))$. In the case of an isotropic rod, one can always perform a continuous rotation of the rod material around its centre line without disturbing the equilibrium. This means that if $\boldsymbol{r}(s)$ satisfies (13) and (14) and $\boldsymbol{d_1}(s)$ satisfies (18), any other configuration $(\boldsymbol{r}(s), \boldsymbol{D_1}(s))$ with $\boldsymbol{D_1}(s) = \cos\alpha \boldsymbol{d_1}(s) + \sin\alpha \boldsymbol{d_2}(s)$ will be in equilibrium, i.e., $\boldsymbol{D_1}(s)$ will satisfy (18). This (continuous) register symmetry has been as source a trouble. It raises the dimension of the solution manifold by one. To solve this problem either additional boundary condition [17, 5] or symmetry group properties [8] were employed. Here we solve this problem at once by decoupling the equations for the centre line (13), (14) from the equation for the material (18). The register symmetry then simply boils down to choosing an initial value for the rotation angle of $\boldsymbol{d_1}(0)$ in the cross section at $s = 0$.

In the case of circularly closed configurations (i.e., rings) there is yet another continuous symmetry: the translational invariance of arc length ($s \to s + \delta$). We have seen in case α of the proof of Section 3.2 that this translational invariance could be used to isolate solutions: the solutions that starts ($s = 0$) at a point of minimal or maximal curvature. Hence for a closed solution corresponding to harmonic $n^= = \Omega$, we will isolate 2Ω discrete solutions among the S^1 continuum.

Once a first solution is computed, one can reconstruct the continuum in the following way. Associated to any closed solution with $(m_z, m_{x0}, \theta_0, f)$ and $m_{y0} = 0$, there are solutions of the same shape with the same m_z and f but with $\widetilde{m}_{y0} \neq 0$, $\tilde{\theta}_0$ and $\widetilde{m}_{x0}$ such that:

$$m_{x0} \sin\theta_0 + m_z \cos\theta_0 \;=\; m_3 = \widetilde{m}_{x0} \sin\tilde{\theta}_0 + m_z \cos\tilde{\theta}_0 \quad \text{and} \tag{91}$$

$$\frac{1}{2}(m_{x0}^2 + m_z^2) + f \cos\theta_0 \;=\; I_2 = \frac{1}{2}(\widetilde{m}_{x0}^2 + \widetilde{m}_{y0}^2 + m_z^2) + f \cos\tilde{\theta}_0. \tag{92}$$

Hence for circularly closed configurations, the two continuous symmetries (register and translational invariance of arc length) yield a T^2 torus of solutions associated with each equilibrium solution. With the reduction presented here, we select 2Ω isolated points on this torus.

4.6. ROD WITH NO TWIST: THE $m_3 = 0$ PATHS

Another interesting subset of the clamped solutions are rods with $m_3 = 0$: rods held such that no twist can be assignated to it, like held in sleeves. Of course an important subset on these solutions are the planar elastica but we stress here that untwisted 3D solutions (clamped or not) also exist. For example, as first established in [19], a rod held with sleeves will bifurcate in 3D at a certain point A along the 1st planar infexional elastica ($A = \{m_z, m_{x0}, \theta_0, f\} = \{0, 1.32, \pi, 1.235\}$ and $d = 0.3715$) and the path will join the $p = 1$ non-inflexional planar elastica at a point B ($B = \{m_z, m_{x0}, \theta_0, f\} = \{0, 1.737, \pi, 0.7\}$ and $d = 0.698$).

In addition to these untwisted 3D solutions, there are twisted planar solutions as well: untwisted is not synonymous to planar (see [7]). All the cases where a rod centre line is not 3D are:

(a) $(I_0, I_1) = (0, 0)$ (planar elastica),
(b) twisted planar rings (under force and non constant moment),
(c) twisted straight rod under force and constant moment,
(d) twisted straight rod under no force and constant moment.

These cases can be found in Tables II–IV.

Table II. Depending on initial conditions $\boldsymbol{d_3}(0)$ and parameters $\boldsymbol{m}_K$ and f, here are all possible shapes when there is no force. In the first 3 columns, when the name of a parameter appears standing alone (e.g., d_{3x0}), this means that its value is not restricted at this point. Case 3 can never be clamped

$\boldsymbol{d_3}(0)$	$\boldsymbol{m}_K$	$\boldsymbol{f}$	Remark or additional cond.	I_0	I_1 (m_3)	Shape	Remark on shape
d_{3x0} d_{3y0} d_{3z0}	0 0 0	0 0 0	$\boldsymbol{m}_K = 0$	0	0	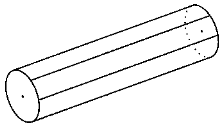	$\boldsymbol{m}(s) \equiv 0$ $\boldsymbol{d_3}(s) \equiv cte$
d_{3x0} d_{3y0} 0	0 0 $m_z \neq 0$	0 0 0	$\boldsymbol{m}_K \neq 0$	0	0	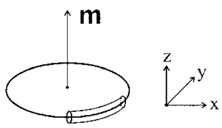	$\boldsymbol{m}(s) \equiv cte$ $d_{3z}(s) \equiv 0$
d_{3x0} d_{3y0} d_{3z0}	0 0 $m_z \neq 0$	0 0 0	$\lvert d_{3z0}\rvert < 1$	0	$\neq 0$	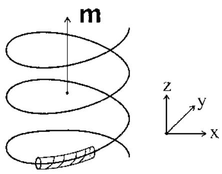	$\boldsymbol{m}(s) \equiv cte$ helix 3D
0 0 ± 1	0 0 $m_z \neq 0$	0 0 0	$d_{3z0} = \pm 1$	0	$\neq 0$	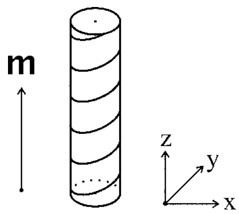	$\boldsymbol{m}(s) \equiv cte$

Table III. Depending on initial conditions $\boldsymbol{d_3}(0)$ and parameters $\boldsymbol{m}_K$ and f, here are the different shapes when there is a force but no initial moment. We always choose the y axis such that $d_{3y0} = 0$. In the first 3 columns, when the name of a parameter appear standing alone (e.g., d_{3x0}), this means that its value is not restricted at this point

$\boldsymbol{d_3}(0)$	$\boldsymbol{m}_K$	$\boldsymbol{f}$	Remark or additional cond.	I_0	I_1 (m_3)	Shape	Remark on shape
0 0 ± 1	0 0 0	0 0 $f \neq 0$	$\boldsymbol{m}_K = 0$ $\boldsymbol{d_3}(0) \parallel \boldsymbol{f}$	0	0	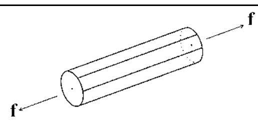	$\boldsymbol{m}(s) \equiv 0$ $d_{3z}(s) \equiv \pm 1$
$d_{3x0} \neq 0$ 0 d_{3z0}	0 0 0	0 0 $f \neq 0$	$\boldsymbol{m}_K = 0$	0	0	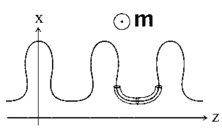	Planar inflex. $m_x(s) \equiv 0$ $m_y(s) \not\equiv 0$ $d_{3y}(s) \equiv 0$

Table IV. Depending on initial conditions $\boldsymbol{d_3}(0)$ and parameters $\boldsymbol{m}_K$ and f, here are the different shapes when there is a force. We always choose the y axis such that $d_{3y0} = 0$. In the first 3 columns, when the name of a parameter (e.g., d_{3x0}) appear standing alone, this means that its value is not restricted at this point

$\boldsymbol{d_3}(0)$	$\boldsymbol{m}_K$	$\boldsymbol{f}$	Remark or additional cond.	I_0	I_1 (m_3)	Shape	Remark on shape
d_{3x0} 0 d_{3z0}	m_{x0} m_{y0} 0	0 0 $f \neq 0$	$d_{3x0}m_{x0} = 0$ $(m_{x0},\ m_{y0})$ $\neq$ $(0, 0)$	0	0	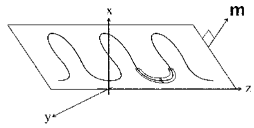	Planar elastica in plane $\perp \boldsymbol{m}_K$ $\boldsymbol{m}(s) \parallel \boldsymbol{m}_K$
d_{3x0} 0 d_{3z0}	m_{x0} m_{y0} 0	0 0 $f \neq 0$	$d_{3x0}m_{x0} \neq 0$	0	$\neq 0$	3D	$I_0 = 0$ but 3D $d_{3y}(s) \not\equiv 0$
0 0 ± 1	0 0 $m_z \neq 0$	0 0 $f \neq 0$	$\boldsymbol{d_3}(0) \parallel \boldsymbol{f}$ $\boldsymbol{m}(0) \parallel \boldsymbol{f}$	$\neq 0$	$\neq 0$	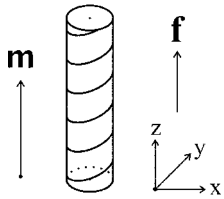	$d_{3x}(s) \equiv 0$ $d_{3y}(s) \equiv 0$ $\boldsymbol{m}(s)$ $=$ $(0, 0, m_z)$
± 1 0 0	$m_{x0} \neq 0$ 0 $m_z \neq 0$	0 0 $f \neq 0$	$f = m_{x0}m_z$	$\neq 0$	$\neq 0$	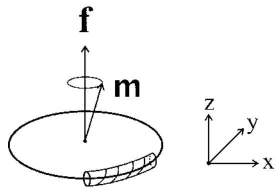	$d_{3z}(s) \equiv 0$
d_{3x0} 0 d_{3z0}	m_{x0} m_{y0} $m_z \neq 0$	0 0 $f \neq 0$	$d_{3x0}m_{x0}$ $=$ $-d_{3z0}m_z$	$\neq 0$	0	3D	no twist but 3D
d_{3x0} 0 d_{3z0}	m_{x0} m_{y0} $m_z \neq 0$	0 0 $f \neq 0$	$d_{3x0}m_{x0}$ $\neq$ $-d_{3z0}m_z$	$\neq 0$	0	3D	general twisted solution

5. Conclusion

In this paper, we have performed a reduction of the Kirchhoff equations describing the equilibrium configurations of the ideal elastica subjected to clamped boundary conditions. This enabled us to factorize of the cubic polynomial (49) and subsequently write the centre line solutions in closed form with the parameters appearing explicitely. This in turn provided us with a set of 2 equations that the 4 paramaters have to fulfil, hence defining the solution manifold of our boundary value problem. We have also shown that the clamped boundary conditions select configurations where the rod shape has a flip symmetry and we conjecture that clamped configurations of rods with non isotropic cross section (i.e. $K_1 \neq K_2$) still exhibit this flip symmetry. Finally, we have provided a classification of the equilibrium configurations by labelling them according to the number of points of maximum and minimum curvature existing along the centre line, the differents sets of configurations with different labels being connected by the set of circularly closed configurations.

Acknowledgements

S.N. acknowledges a grant from the European Science Exchange Programme of the Royal Society, U.K. He also thanks G. Domokos for usefull discussions and J.H. Maddocks for instructive comments.

Appendix

The elliptic integral of the first, second and third kind are defined here:

- $F(\phi, x)$ with $x \in]-\infty; 1[$ is the elliptic integral of the first kind
$$F(\phi, x) = \int_0^\phi \frac{d\theta}{\sqrt{1 - x\sin^2\theta}}. \tag{A.1}$$
Its reciprocal is the Jacobi amplitude function $\mathrm{am}(\varphi, x)$ with $\mathrm{am}(F(\phi, x), x) = \phi$. We note $K(x) \stackrel{\text{def}}{=} F(\pi/2, x)$ the complete elliptic integral of the first kind. Examples: $K(0.2) = 1.65962$ and $K(0.8) = 2.25721$. Note also that $\sqrt{1+x}K(-x) = K(x/1+x)$.

- $E(\phi, x)$ with $x \in] -\infty; 1[$ is the elliptic integral of the second kind
$$E(\phi, x) = \int_0^\phi \sqrt{1 - x\sin^2\theta}\, d\theta. \tag{A.2}$$
We note $\overline{E}(x) \stackrel{\text{def}}{=} E(\pi/2, x)$ the complete elliptic integral of the second kind. Examples: $\overline{E}(0.3) = 1.44536$ and $\overline{E}(0.9) = 1.10477$.
- $\Pi(\mu, \phi, x)$ with $x \in] -\infty; 1[$ is the elliptic integral of the third kind
$$\Pi(\mu, \phi, x) = \int_0^\phi \frac{d\theta}{(1 - n\sin^2\theta)\sqrt{1 - x\sin^2\theta}}. \tag{A.3}$$
We write $\overline{\Pi}(\mu, x) \stackrel{\text{def}}{=} \Pi(\mu, \pi/2, x)$ the complete elliptic integral of the third kind. Example: $\overline{\Pi}(\mu = 0.1, x = 0.2) = 1.75197$.

References

1. S.S. Antman, *Nonlinear Problems of Elasticity*. Springer, New York (1995).
2. A.R. Champneys and J.M.T. Thompson, A multiplicity of localised buckling modes for twisted rod equations. *Proc. Roy. Soc. London A* **452** (1996) 2467–2491.

3. B.D. Coleman and D. Swigon, Theory of supercioiled elastic rings with self contact and its application to DNA plasmids. *J. Elasticity* **60** (2000) 173–221.
4. R.L. Devaney, Reversible diffeomorphisms and flows. *Trans. Amer. Math. Soc.* **218** (1976) 89–113.
5. D.J. Dichmann, Y. Li and J.H. Maddocks, Hamiltonian formulations and symmetries in rod mechanics. In: J.P. Mesirov, K. Schulten and D.W. Sumners (eds), *Mathematical Approaches to Biomolecular Structure and Dynamics*, The IMA Volumes in Mathematics and Its Applications, Vol. 82 (1996) pp. 71–113.
6. G. Domokos, Global description of elastic bars. *Z. angew. Math. Mech.* **74** (1994) T289–T291.
7. G. Domokos, A group-theoretic approach to the geometry of elastic rings. *J. Nonlinear Sci.* **5** (1995) 453–478.
8. G. Domokos and T. Healey, Hidden symmetry of global solutions in twisted elastic rings. *J. Nonlinear Sci.* **11** (2001) 47–67.
9. L. Euler, Methodus inveniendi lineas curvas maximi minimivi propreitate gaudentes. *Opera Omnia I* **24**(1744) 231–297, Füssli, Zürich (1960).
10. M.E. Henderson and S. Neukirch, Classification of the spatial clamped elastica, Numerical continuation of the solution set. *Int. J. Bif. Chaos* (2004) in press.
11. K.A. Hoffman, R.S. Manning and R.C. Paffenroth, Calculation of the stability index in parameter-dependent calculus of variations problems: Buckling of a twisted elastic strut. *SIAM J. Appl. Dyn. Systems* **1**(1) (2002) 115–145.
12. A.A. Ilyukhin, *Spatial Problems of Nonlinear Theory of Elastic Rods*. Naukova Dumka, Kiev (1979) (in Russian).
13. S. Kehrbaum, Hamiltonian formulations of the equilibrium conditions governing elastic rods: Qualitative analysis and effective properties. PhD Thesis, University of Maryland, College Park (1997).
14. S. Kehrbaum and J.H. Maddocks, Elastic rods, rigid bodies, quaternions and the last quadrature. *Phil. Trans. Roy. Soc. London A* **355** (1997) 2117–2136.
15. L.D. Landau and E.M. Lifshitz, *Theory of Elasticity*, *Course of Theoretical Physics*, Vol. 7, 3 edn. Pergamon Press, Oxford (1986).
16. J. Langer and D.A. Singer, Lagrangian aspects of the Kirchhoff elastic rod. *SIAM Rev.* **38**(4) (1996) 605–618.
17. Y. Li and J.H. Maddocks, On the computation of equilibria of elastic rods, part I: Integrals, symmetry and a Hamiltonian formulation. *J. Comput. Phys.* Preprint (1994).
18. A.E.H. Love, *A Treatise on the Mathematical Theory of Elasticity*, 4th edn. Dover, New York (1944).
19. J.H. Maddocks, Stability of nonlinearly elastic rods. *Arch. Rational Mech. Anal.* **85**(4) (1984) 180–198.
20. S. Neukirch, G.H.M van der Heijden and J.M.T. Thompson, Writhing instabilities of twisted rods: From infinite to finite length. *J. Mech. Phys. Solids* **50** (2002) 1175–1191.
21. M. Nizette and A. Goriely, Toward a classification of Euler–Kirchhoff filaments. *J. Math. Phys.* **40** (1999) 2830–2866.
22. Y. Shi and J.E. Hearst, The Kirchhoff elastic rod, the nonlinear Schrödinger equation and DNA supercoiling. *J. Chem. Phys.* **101** (1994) 5186–5200.
23. E.L. Starostin, Three-dimensional shapes of looped DNA. *Meccanica* **31** (1996) 235–271.
24. D. Swigon, Configurations with self contact in the theory of the elastic rod model for DNA. PhD Thesis, Rutgers State University of New Jersey, U.S.A. (1999).
25. H. Tsuru, Equilibrium shapes and vibrations of thin elastic rod. *Journal of the Physical Society of Japan* **56**(7) (1987) 2309–2324.
26. G.H.M. van der Heijden and J.M.T. Thompson, Helical and localised buckling in twisted rods: A unified analysis of the symmetric case. *Nonlinear Dynamics* **21** (2000) 71–79.